Progress In Electromagnetics Research Letters, Vol. 68, 127–133, 2017

A Compact High-Gain Vivaldi Antenna with Improved Radiation Characteristics

Jingya Zhang, Shufang Liu*, Fusheng Wang, Zhanbiao Yang, and Xiaowei Shi

Abstract—In this paper, a miniaturized Vivaldi antenna for C- to X-bands is proposed and fabricated. An H-Shaped Resonator (HSR) and transverse slot structures are employed in this design, which improve the gain through the entire band, especially at the high frequency band. These simulated results show that the modified Vivaldi antenna has a maximum gain increment of 4 dBi and peak gain of 9.9 dBi. Furthermore, the modified Vivaldi antenna has narrower half-power beam width (HPBW), higher front-to-back ratio (FBR) and better radiation characteristics. The measured results are in good agreement with the simulated ones.

1. INTRODUCTION

Vivaldi antenna, a broadband antenna that was originally introduced by Gibson in 1979, not only satisfies the requirement of UWB, but also has a planar structure, low profile and high efficiency in contrast to other UWB antennas [1]. However, the most referenced antennas are relatively large in size [2], which cannot fit our need for the limited space. In recent years, with the miniaturization of the Vivaldi antenna, the gain decreases sharply [3, 4]. In [3], the small antipodal Vivaldi antenna has a wide bandwidth from 3.1 to 10.6 GHz, but this design is at the cost of low gain, whose gain is only 5.2 dBi. In order to improve the gain, some approaches have been proposed. Using array of Vivaldi antenna [5] is the conventional way to obtain high gain, but it is complicated and bulky for compact wireless systems. In [6], Y-shaped slots are etched on the radiation patch to improve radiation characteristics. However, they are complex, and more parameters need to be optimized. Furthermore, it is found that the radiation pattern begins to deteriorate at 12 GHz. The higher the frequency is, the wider the HPBW becomes. In [7], HSR structures are loaded to narrow the HPBW and improve the pattern bandwidth. The measured results show that the HSR-loaded antenna has a high gain.

In this paper, a compact high-gain Vivaldi antenna is designed. Firstly, to focus on the energy in the end-fire direction and improve the gain, the HSR structures are applied in front of the antenna's aperture. Secondly, in order to improve the FBR and enhance the gain, the transverse slots are etched on the radiation patch. Finally, both the loaded antenna and the unloaded one are fabricated and measured. A comparison is made between the simulated results and the measured ones.

The paper proceeds to discuss the antenna configuration, HSR and transverse slot structures in Section 2. Section 3 discusses the simulated and measured results of the loaded and unloaded antennas. Finally, a conclusion is drawn in Section 4.

2. ANTENNA ANALYSIS AND DESIGN

A compact high-gain antenna is designed as shown in Figure 1. Rogers RT/duroid 5880 is used as its substrate with a relative permittivity of 2.2 and thickness of 1 mm. The antenna consists of five parts:

Received 15 March 2017, Accepted 27 April 2017, Scheduled 22 June 2017

* Corresponding author: Shufang Liu (shfliu999@tom.com).

The authors are with the National Key Laboratory of Antennas and Microwave Technology, Xidian University, Xi'an, Shanxi 710071, P. R. China.

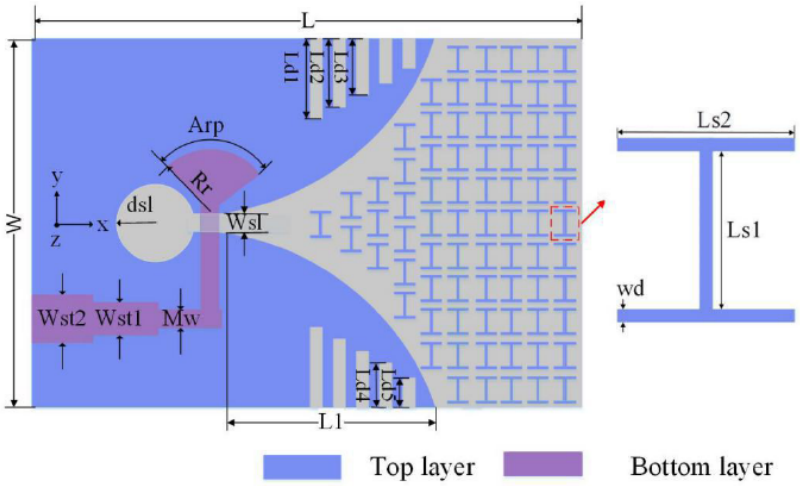

Figure 1. Geometry of the proposed antenna.

dielectric substrate, metal ground plane, feeding microstrip transmission line, HSR and transverse slot structures. The exponential tapered slot on the ground plane can be expressed as:

$$y = ae^{Rx} + b$$
$$a = \frac{y_2 - y_1}{e^{Rx_2} - e^{Rx_1}}$$
$$b = \frac{y_1 e^{Rx_2} - y_2 e^{Rx_1}}{e^{Rx_2} - e^{Rx_1}}$$

where (x_1, y_1), (x_2, y_2) are the peak and bottom points of the exponential tapered shape, respectively, and R is the exponential factor of the antenna [8].

To excite the proposed antenna, a microstrip-to-slotline transition balun is employed, as shown in Figure 1. By connecting it to the SMA connector, it can excite the Vivaldi antenna with a broadband impedance matching. However, we find that the gain of the unloaded antenna is relatively low in the end-fire direction ($+x$ axis). As shown in Figure 2, the gains at the point ($\theta = 90°$ $\varphi = 0°$) are 6.9 dBi at 10 GHz, 4.6 dBi at 12 GHz, and 3.3 dBi at 13.5 GHz, respectively. Moreover, as shown in Figure 2, with the increase of frequency, the radiation pattern becomes worse, and the FBR decreases sharply.

It can be seen from the simulated results that the unloaded antenna has a scattered beam, which

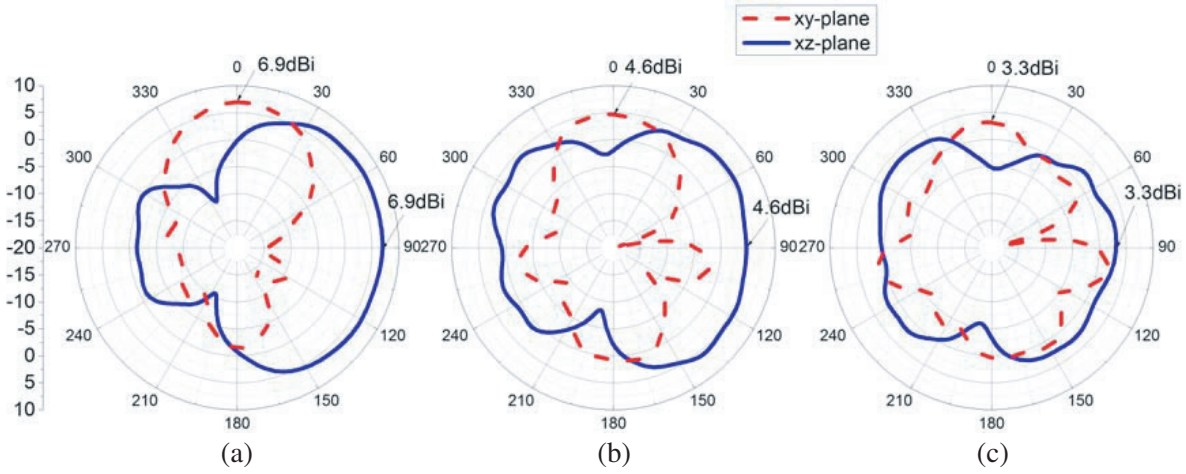

Figure 2. Simulated radiation patterns of the unloaded antenna. (a) 10 GHz. (b) 12 GHz. (c) 13.5 GHz.

leads to bad radiation pattern and low gain. So a method of focusing beam is required to enhance the performance of the antenna. Based on Snell's law $n_s \cdot \sin\theta_s = n_0 \cdot \sin\theta_0$, which is shown in Figure 3. When the refractive index (n_s) of the substrate gets larger, with the same incident angle θ_s, the refracting angle θ_0 gets larger, so the beam can be focused on the end-fire direction ($+x$ axis), and a high gain can be received [9]. For a substrate with a larger refractive index, a metamaterial composed of the substrate given above and the HSR structure (Figure 1) is used here. The most common and effective way to extract parameters of metamaterial is used here to guide the design [9–12].

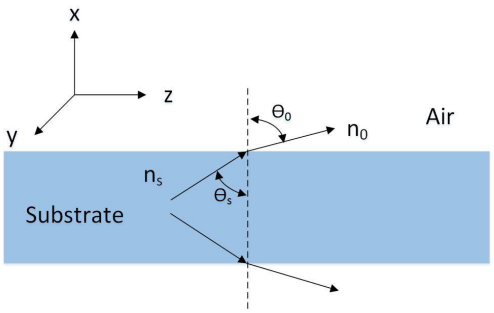

Figure 3. Electromagnetic wave transmitting sketch map.

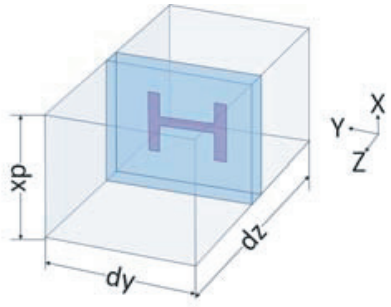

Figure 4. The simulation model of HSR unit.

The HFSS model for extracting the refractive index of the HSR unit is shown in Figure 4. And the simulated S-parameters are shown in Figure 5. HSR structures are employed for controlling the refractive index. Figure 5 shows clearly that the HSR structure has a great effect on the transmission characteristics. The refractive index of the dielectric with the HSR unit loaded is higher than the unloaded dielectric. So the high gain of the antenna with HSR is achieved.

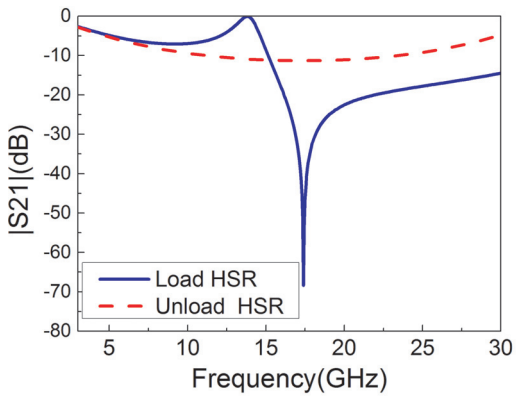

Figure 5. Simulated S-parameters of the HSR unit.

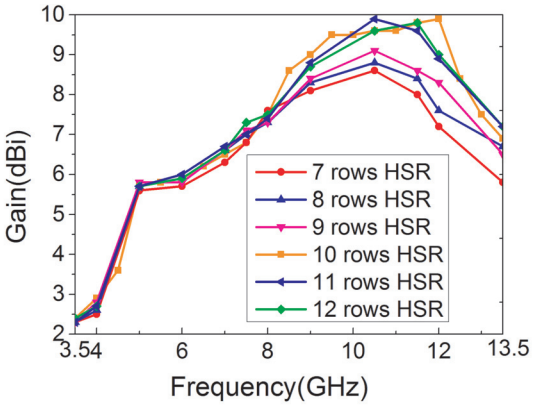

Figure 6. Influence of different rows of HSR on antenna gain.

The dependence of the different rows of HSR on the antenna gain is depicted in Figure 6. Obviously, as the number of rows increases, the gain also increases. However, when the rows exceed 10, the increase is less obvious. To keep the antenna compact, we choose ten rows of HSR as a compromise.

To improve radiation characteristics of the antenna without extension in dimension, five symmetric transverse slots are etched on both sides of the metal patch. Each slot operates as an RLC resonator. Five slots with varied length are added to constrain the surface current to the vicinity of the tapered slot line. Meanwhile, they change the flow direction of the edge current and improve the contribution of the edge current to the radiation in the direction of end-fire, so high gain is obtained.

3. RESULTS AND DISCUSSION

The dimensions of the antenna are optimized to achieve good impedance matching and high gain. The final optimal dimensions are obtained and listed in Table 1. To validate the design, both prototypes of the unloaded and loaded antennas are fabricated and measured. Photographs of the antennas and the testing environment are shown in Figure 7.

The antennas are measured with the Agilent Technologies MS46322A vector network analyzer. Figure 8 shows the simulated and measured S_{11}. The -10 dB impedance bandwidths are 121.9% (3.3–13.6 GHz) for the unloaded antenna and 123.3% (3.3–13.9 GHz) for the loaded one. It is clear that good agreement between the simulated and measured S_{11} is obtained. The HSR and transverse slots have little effect on the impedance matching.

Table 1. Dimensions of proposed antenna.

Parameters	Values /mm	Parameters	Values /mm	Parameters	Values /mm	Parameters	Values /mm	Parameters	Values /mm	Parameters	Values /mm
W	29.0	dsl	3.8	Arp	100 deg	L	38.0	Mw	1.4	$Ls1$	1.6
Rr	4.1	$Wst1$	2.2	$Wst2$	3.0	$L1$	14.5	$Ld1$	9.0	$Ls2$	1.85
$Ld2$	8.1	$Ld3$	7.2	$Ld4$	6.3	$Ld5$	5.4	Wsl	0.85	wd	0.25

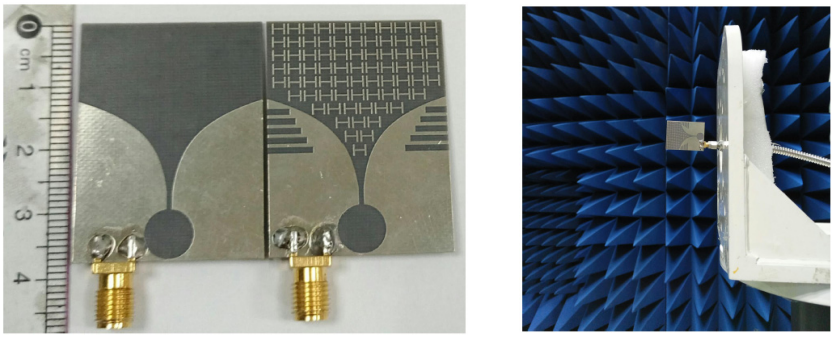

(a) (b)

Figure 7. (a) A prototype of the unloaded antenna and loaded antenna; (b) testing environment.

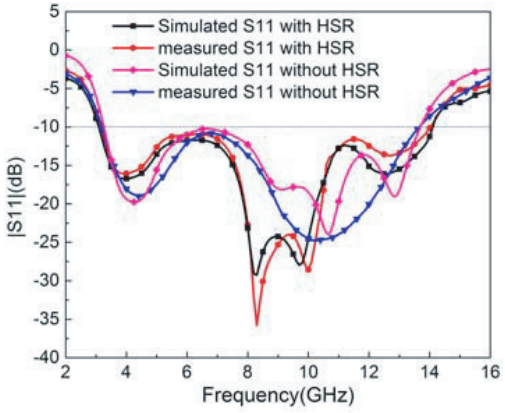

Figure 8. Measured and simulated S_{11} curves for both antennas.

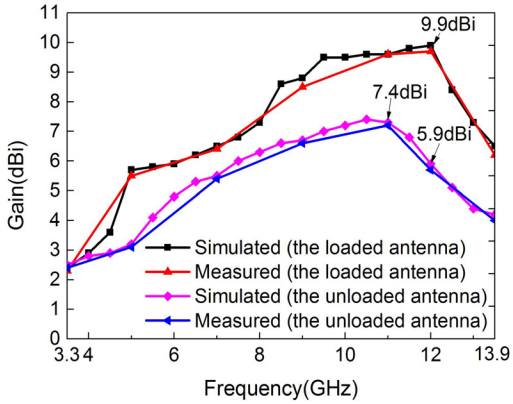

Figure 9. Measured and simulated maximum gain curves for both antennas.

Figure 9 shows the simulated and measured gain curves in the end-fire direction ($+x$ axis). Within the operating frequency band, the measured gain is about 2.4–9.9 dBi for the loaded antenna and 2.4–7.4 dBi for the unloaded one. As shown in Figure 9, from 3.3 to 8 GHz, the gain increases by about 1 dBi, and the maximum is 2.5 dBi. However, from 8 to 13.9 GHz, the increment of the gain is above 2 dBi, and the maximum is 4 dBi. Here a gain increment of about 1–4 dBi is obtained.

Figure 10 gives the surface current distributions of both the antennas. We can clearly observe that there is nonnegligible surface current around these slots and the HSR structures.

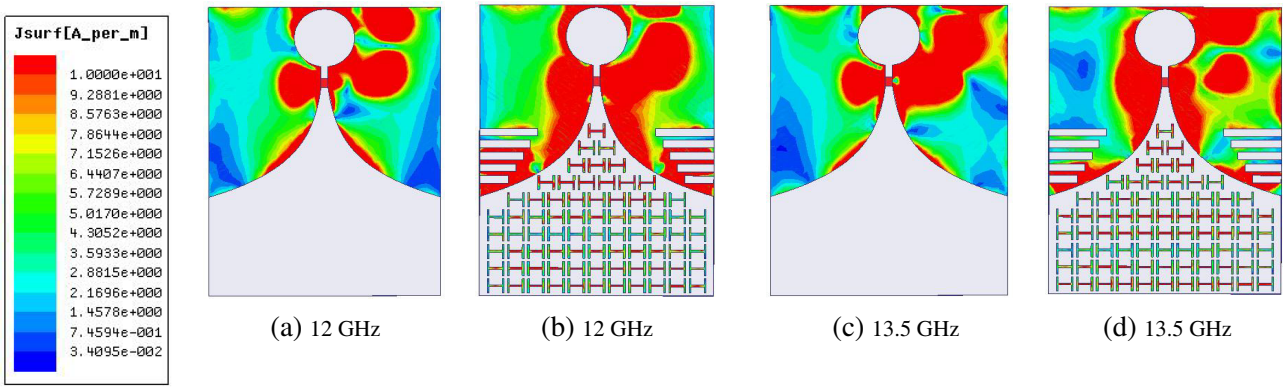

Figure 10. Surface current distribution of the both antennas.

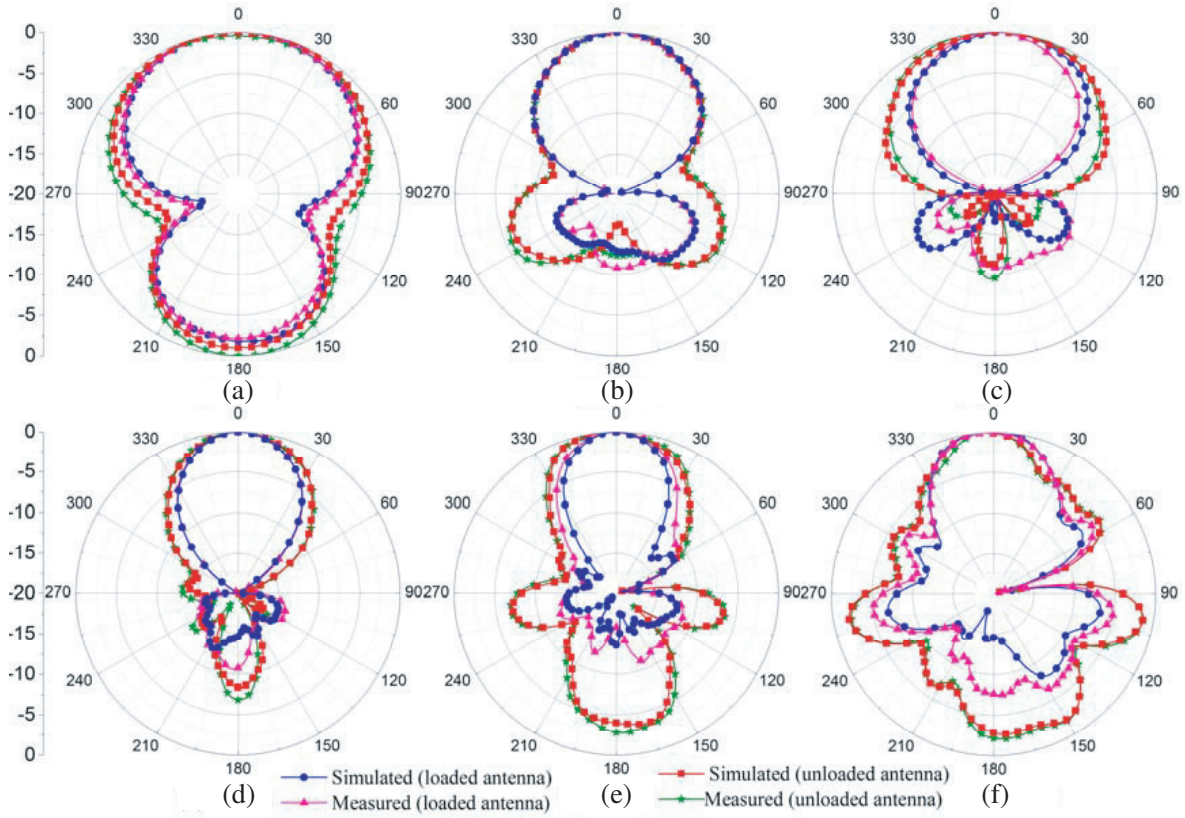

Figure 11. Measured and simulated radiation patterns for the unloaded antenna and the loaded antenna at 4, 6, 8, 10, 12 and 13 GHz in xy-plane. (a) 4 GHz. (b) 6 GHz. (c) 8 GHz. (d) 10 GHz. (e) 12 GHz. (f) 13 GHz.

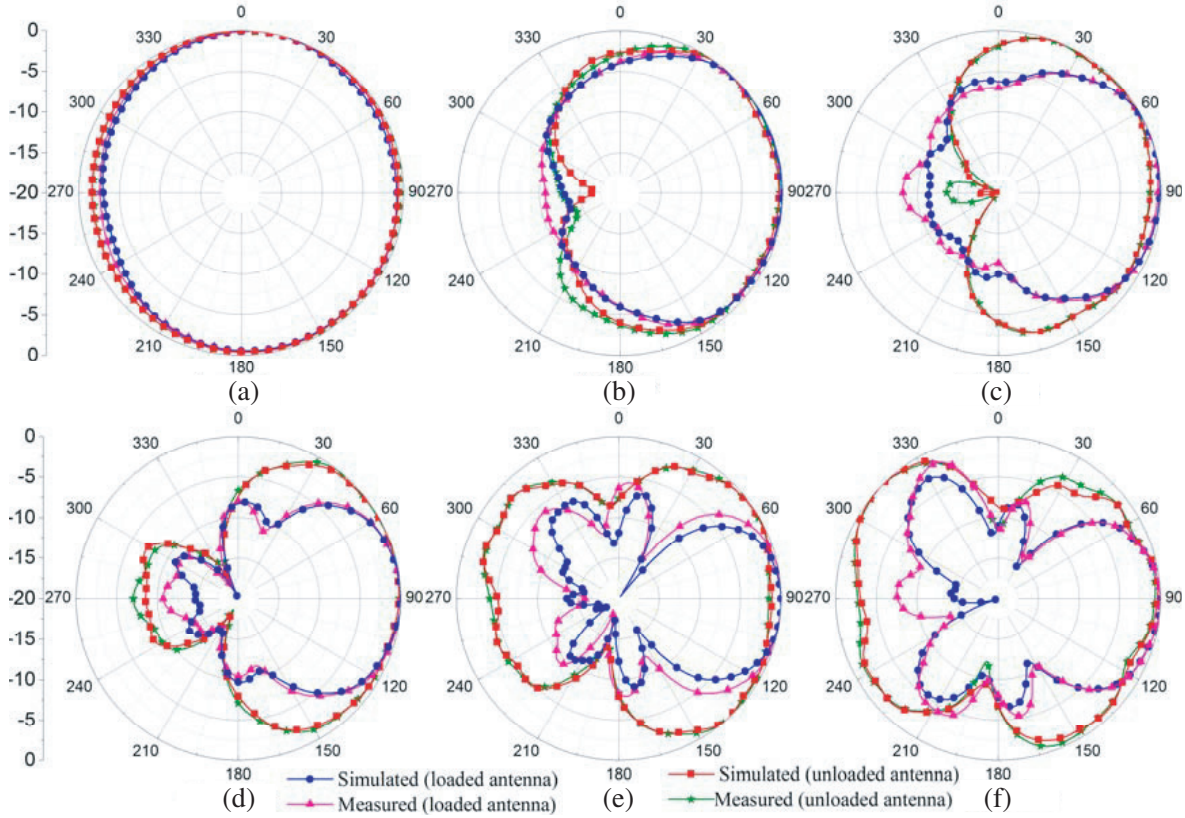

Figure 12. Measured and simulated radiation patterns for the unloaded antenna and the loaded antenna at 4, 6, 8, 10, 12 and 13 GHz in xz-plane. (a) 4 GHz. (b) 6 GHz. (c) 8 GHz. (d) 10 GHz. (e) 12 GHz. (f) 13 GHz.

The radiation patterns of both antennas in xy-plane and xz-plane are shown in Figures 11 and 12, respectively. Compared with the unloaded one, the modified antenna can achieve unidirectional radiation patterns with stable radiation direction. The main beam begins to converge, and the HPBW becomes narrow. The HPBW decreases more than 50 degrees in xz-plane and more than 12 degrees in xy-plane at the high frequency. In addition, the FBR is improved significantly, especially at the high frequency band. The results of the analysis are shown in Table 2. In conclusion, the loaded antenna has more focused beam, higher gain and better radiation patterns.

Table 2. Radiation properties of the both antennas.

Type	Frequency/GHz		6	7	8	9	10	11	11.5	12	12.5	13	13.5
Unloaded antenna	FBR/dBi		16.1	13.7	16.4	7.7	8.3	4.5	3.9	3.9	3.7	2.8	3
	HPBW/°	xy-plane	68	73	100	75	60	52	53	60	60	63	52
		xz-plane	150	199	182	164	147	130	133	147	152	128	112
Loaded antenna	FBR/dBi		15.9	14.4	15.3	13.8	14.8	15.1	21.6	13.6	9.4	14.6	7.1
	HPBW/°	xy-plane	67	71	97	45	45	40	41	40	48	48	40
		xz-plane	145	133	107	91	82	76	70	71	70	70	59

4. CONCLUSION

In this paper, a compact broadband high gain Vivaldi antenna is designed and fabricated. The results show that the loaded antenna has a gain about 2.4–9.9 dBi over the whole working band (3.3–13.9 GHz). Compared with the unloaded one, a gain increment about 1–4 dBi is achieved. Moreover, the results show that HPBW of the loaded antenna decreases more than 12 degrees in xy-plane and 50 degrees in xz-plane compared to the conventional design. It is proved that the improved antenna has the characteristics of higher gain, higher FBR and better radiation patterns. The advantages make this improved Vivaldi antenna valuable in the wireless communication and the radar systems.

ACKNOWLEDGMENT

This work is supported by the Fundamental Research Funds for the Central Universities JB150211 and NSFC61301066.

REFERENCES

1. Molaei, A., M. Kaboli, S. A. Mirtaheri, and M. S. Abrishamian, "Dielectric lens balanced antipodal Vivaldi antenna with low cross-polarisation for ultra-wideband applications," *IET Microwaves, Antennas and Propagation*, Vol. 8, 1137–1142, 2014.
2. In, D. M., M. J. Lee, D. Kim, et al., "Antipodal linearly tapered slot antenna using unequal half-circular defected sides for gain improvements," *Microwave and Optical Technology Letters*, Vol. 8, No. 54, 1963–1965, 2012.
3. Hood, A. Z., T. Karacolak, and E. Topsakal, "A small antipodal Vivaldi antenna for ultrawide-band application," *IEEE Antennas Wireless Propag. Lett.*, Vol. 7, 656–660, 2008.
4. Abayaje, F. and P. Febvre, "A customized reduced size antipodal Vivaldi antenna used in wireless baseband transmission for short-range communication," *AEU — International Journal of Electronics and Communications*, Vol. 70, 1684–1691, 2016.
5. Reid, E. W., L. Ortiz-Balbuena, A. Ghadiri, and K. Moez, "A 324-element Vivaldi antenna array for radio astronomy instrumentation," *IEEE Trans. Antennas Propag.*, Vol. 61, No. 1, 241–249, 2012.
6. Liu, H.-X., J. Gao, S.-J. Li, and D. Zhang, "Y-shaped aperture loaded miniaturized ultra-wide band Vivaldi endfire antenna," *Journal of Air Force Engineering University (Natural Science Edition)*, Vol. 16, No. 2, 73–77, 2015.
7. Wang, H., S.-F. Liu, L. Chen, W.-T. Li, and X.-W. Shi, "Gain enhancement for broadband vertical planar printed antenna with H-shaped resonator structures," *IEEE Trans. Antennas Propag.*, Vol. 62, 4411–4415, 2014.
8. Herzi, R., H. Zairi, and A. Gharsallah, "Reconfigurable Vivaldi antenna with improved gain for UWB applications," *Microwave and Optical Technology Letters*, Vol. 58, 490–494, 2016.
9. Ziolkowski, R. W., "Design, fabrication, and testing of double negative metamaterials," *IEEE Trans. Antennas Propag.*, Vol. 51, 1516–1529, 2003.
10. Smith, D. R., D. C. Vier, T. Koschny, and C. M. Soukoulis, "Electromagnetic parameter retrieval from inhomogeneous metamaterials," *Phys. Rev. E*, Vol. 71, 036617, 2005.
11. Chen, L. and X. Shi, "Study on high-gain and directional antennas based on metamaterials," XiDian University, Xi'an, 2015.
12. Bai, J., S. Shi, and D. W. Prather, "Modified compact antipodal Vivaldi antenna for 4–50-GHz application" *IEEE Trans. Microw. Theory Tech.*, Vol. 59, No. 4, 1051–1057, 2011.